Electronic Supplementary Material (ESI) for Chemical Communications.
This journal is © The Royal Society of Chemistry 2024

Supporting Information

Strategic Structure Modulation of Novel Quinoxaline-Derived Liquid Organic Hydrogen Carriers for Enhanced Dehydrogenation Kinetics

*Li Liu, Ting Zhu, Jiaqi Li, Can Wang, Yinheng Zhao, Ming Yang, Hansong Cheng, Yuan Dong**

Hubei Hydrogen Energy Technology Innovation Center, Faculty of Materials Science and Chemistry, China University of Geosciences, Wuhan 430074, P R China

*Corresponding authors. E-mail address: dongyuancug@163.com.

This file includes:

Number of pages: 27

Number of tables: 6

Number of figures: 3

1. Experimental

1.1 Materials

The experimental materials used in this paper were all commercially purchased reagents. The hydrogenation reactants, including 2-methylquinoline (2-MQL), 2-methylquinoxaline (2-MQX) and 2,3-dimethylquinoxaline (2,3-DMQX), were purchased from Alfa Aesar Co. Ltd. The commercial 5 wt% Ru/Al_2O_3 catalysts and 5 wt% Pd/Al_2O_3 catalysts were provided by Shaanxi Kaida Chemical Co., LTD. The fully hydrogenated products, 10H-2-methylquinoline (10H-2-MQL), 10H-2-methylquinoxaline (10H-2-MQX) and 10H-2,3-dimethylquinoxaline (10H-2,3-DMQX) were achieved by hydrogenation of respective raw materials catalyzed by commercial 5 wt% Ru/Al_2O_3 in a stainless-steel high-pressure reactor (Shanghai LABE instrument LB250). In order to obtain fully hydrogenated products, all hydrogenation reactions were carried out at elevated reaction temperature and hydrogen pressure. Prior to the reaction, the reactor was purged with hydrogen multiple times to remove air from the system. The temperature was then raised to 180 °C, and the hydrogenation reaction was carried out at a hydrogen pressure of 9 MPa with a stirring speed of 600 rpm. Liquid samples were periodically extracted from the reactor and analyzed using a GC-MS (Agilent 7890-5975 C). The reaction was stopped after confirmation of complete hydrogenation was obtained through GC-MS analysis. The liquid samples diluted with hexane (1:100 wt/wt) were injected by an autosampler. The injector temperature was set as 300 °C in the whole run. Helium was used as a carrier gas at a constant flow rate of 20 ml/min. Liquid mixtures were separated by the MS

capillary column (DB-17ms, 30 m×250 μm × 0.25 μm) with programming the oven in two temperature-rising stages. Initial temperature of 95 °C was followed by an increase of 8 °C/min to 180 °C and maintained for 3 min.

1.2 Catalytic dehydrogenation process

The dehydrogenation reactions of all three LOHCs was conducted in a 250 ml two-necked flask containing 1g of LOHC and 0.2g of the selected catalyst. To explore the hydrogen release performance of various LOHC materials, we utilized the fully hydrogenated products obtained in batches during the hydrogenation process as the dehydrogenation feedstock. A 5 wt% Pd/Al_2O_3 catalyst was employed as the dehydrogenation catalyst for comparative analysis. Given that dehydrogenation is an endothermic reaction, temperature plays a crucial role in determining the dehydrogenation rate. Hence, our dehydrogenation experiments aimed to primarily investigate the impact of temperature on the dehydrogenation performance and kinetics. The influence of temperature on dehydrogenation rate was investigated by adding 5 wt% Pd/Al_2O_3 within the temperature range of 180 °C - 210 °C. A small amount liquid samples were also periodically extracted from the reactor and analyzed using GC-MS (Agilent 7890-5975 C).

1.3 Calculation of Activation Energy

In order to calculate the activation energy for each stage of quinoxaline-based LOHCs dehydrogenation, we fitted the reaction results at each temperature by MATLAB software and used non-linear least squares to calculate the equilibrium constants k_1 and k_2 for each level of

the reaction. The specific calculation equations are as follows:

In the following equations, the concentrations of 10H-X, 4H-X, and 0H-X are defined as A, B, and C, respectively, t is real reaction time.

$$A \xrightarrow{k_1} B \xrightarrow{k_2} C \tag{1}$$

$$-\frac{d[A]}{dt} = k_1[A] \tag{2}$$

$$\frac{d[B]}{dt} = k_1[A] - k_2[B] \tag{3}$$

$$\frac{d[C]}{dt} = k_2[B] \tag{4}$$

The Arrhenius curves for each stage of the reaction were obtained by plotting the natural logarithm of k_1 and k_2 against 1/T, respectively. The activation energy of each stage of the reaction is calculated according to the Arrhenius equation:

$$\ln k = \frac{-E_a}{RT} + C \tag{5}$$

Here, R is the molar gas constant, $J \cdot mol^{-1} \cdot K^{-1}$; T is the reaction temperature, K; Ea is the apparent activation energy, $J \cdot mol^{-1}$.

No uncommon hazards are noted in all experiments.

1.4 DFT Calculations

1.4.1 Calculations of dehydrogenation temperatures

Model construction and calculations of quinolines were completed using Material studio software, and spin polarization calculations for each structure were performed using the DMol^3 module based on density generalized function theory. The basic parameters of the calculations are as follows: the exchange-correlation generalized function is PW91 in the generalized gradient function GGA, the SCF accuracy is 2×10^{-5} Ha, the maximum force convergence is 0.004 Ha/Å, and the maximum displacement convergence accuracy is 0.005 Å.

The thermodynamic data such as Internal energy, Enthalpy, Entropy and Gibbs free energy of each structure were obtained by calculations to obtain the dehydrogenation reaction temperature of quinolines according to the reaction equation (6). Where, $C_xH_{y+2n}N_z$ represents the hydride of quinoline analogs, $C_xH_yN_z$ represents quinoline analogs, and n H_2 represents the release of stoichiometric number of hydrogen.

$$C_xH_{y+2n}N_z \rightarrow C_xH_yN_z + n\,H_2 \tag{6}$$

For a certain level of dehydrogenation reaction of CxHy+2nNz, the equilibrium constant K and Gibbs free energy change ΔG satisfy the relationship of Eq. (7). In addition, the equilibrium constant K and the conversion ratio are obtained by Eqs. (8) and (9), respectively.

$$\Delta G(T) = -RT\,lnK \tag{7}$$

$$K = \frac{[C_xH_yN_z]\cdot[P_{H_2}]^n}{[C_xH_{y+2n}N_z]} \tag{8}$$

$$X = \frac{[C_xH_yN_z]}{[C_xH_{y+2n}N_z]} \tag{9}$$

It can be obtained by the derivation of Eqs. (7)-(9):

$$\Delta G(T) = -RT(\ln X + n\ln P_{H_2}) \tag{10}$$

The ΔG(T) at different temperatures T can be determined from the above thermodynamic data, so that the function curve $f_1(T)$ can be plotted as a function of temperature T for ΔG(T) when P_{H_2} is 1 atm. When the dehydrogenation reaction (1) reaches catalytic equilibrium, the intersection of the function curve $f_1(T)$ with the temperature T axis is the dehydrogenation temperature T_d. Similarly, assuming that each step of the dehydrogenation is a complete dehydrogenation reaction (X=100%), the function curves $f_P(T)$ can be obtained for different

conditions of hydrogen partial pressure. However, the intersection of the curves $f_1(T)$ and $f_P(T)$ is the equilibrium temperature (T_d) of the dehydrogenation reaction for a definite conversion ratio X (assuming 100% conversion) and a given hydrogen pressure P_{H_2}.

1.4.2 Calculation of Hydrogenation heat

Hydrogenation of quinoline molecules proceeds as in Eq. (11). The heat of hydrogenation of LOHCs was obtained by combining the energies of each molecule obtained from DMol[3] calculations according to Eq. (12). Where E_{H_2} is the calculated energy of H_2, $E_{C_xH_yN_z}$ is the energy of $C_xH_yN_z$, and $E_{C_xH_{y+2n}N_z}$ is the energy of $C_xH_{y+2n}N_z$.

$$C_xH_yN_z + n\,H_2 \rightarrow C_xH_{y+2n}N_z \tag{11}$$

$$Hydrogenation\ heat = \frac{E_{C_xH_{y+2n}N_z} - E_{C_xH_yN_z} - nE_{H_2}}{n} \tag{12}$$

1.4.3 Calculation of hydrogen storage molecule adsorption on Pd(111) surface

The conformational structures of different molecules for the molecular stepwise dehydrogenation of 10H-X LOHCs were constructed by Materials Studio software. The reaction pathways for the stepwise dehydrogenation of 10H-X were deduced by comparing the energies of the different isomeric conformations, and the detailed data are listed in Table S1-S3.

Pd(111) facet exhibits a low surface energy with the closest packed, making them thermodynamically favorable and highly reactive compared to other facets[1, 2]. Stable 10H-X, 8H-X, 6H-X, 4H-X, 2H-X, and X structural models were displayed in Table S1-S3 and adsorbed onto the most stable (111) crystal plane of the Pd metal. The effect of the number

of N atoms and side groups on the rate of dehydrogenation was investigated by analyzing adsorption energy (E_{ads}) and reaction energy (ΔH) data. The Pd metal was sectioned along the (111) facets and expanded into 5 × 5 supercells. A vacuum layer of 15 Å was added to avoid interactions of periodic atoms in the z-direction. The lattice parameter of the Pd(111)-p(5 × 5) flat plate structure is 13.76 × 13.76 × 21.74, and the four-layer structure includes 100 Pd atoms. The Pd(111)-p(5 × 5) structure is optimized and the energy is calculated by fixing the lower two layers of Pd atoms while the surface two layers of Pd atoms are relaxed.

The adsorption energy (E_{ads}) and reaction energy (ΔH) are calculated as follows:

$$E = E_{m/slab} - E_{slab} - E_{m} \tag{13}$$

$E_{m/slab}$, E_{slab}, and E_{m} respectively represent the energy of the adsorbate on Pd(111)-p(5×5) slab, the energy of the slab itself, and the energy of the adsorbate.

$$\Delta H = E_{C_xH_yN_z} + nE_{H_2} - E_{C_xH_{y+2n}N_z} \ (n = 1 - 5) \tag{14}$$

$E_{C_xH_yN_z}$ represents the energy of hydrogen-poor molecules on Pd(111) surfaces; $E_{C_xH_{y+2n}N_z}$ refers to the energy of hydrogen-rich molecules on Pd(111) surfaces; E_{H_2} denotes the energy of hydrogen molecules.

2. Supplementary Figures and Tables

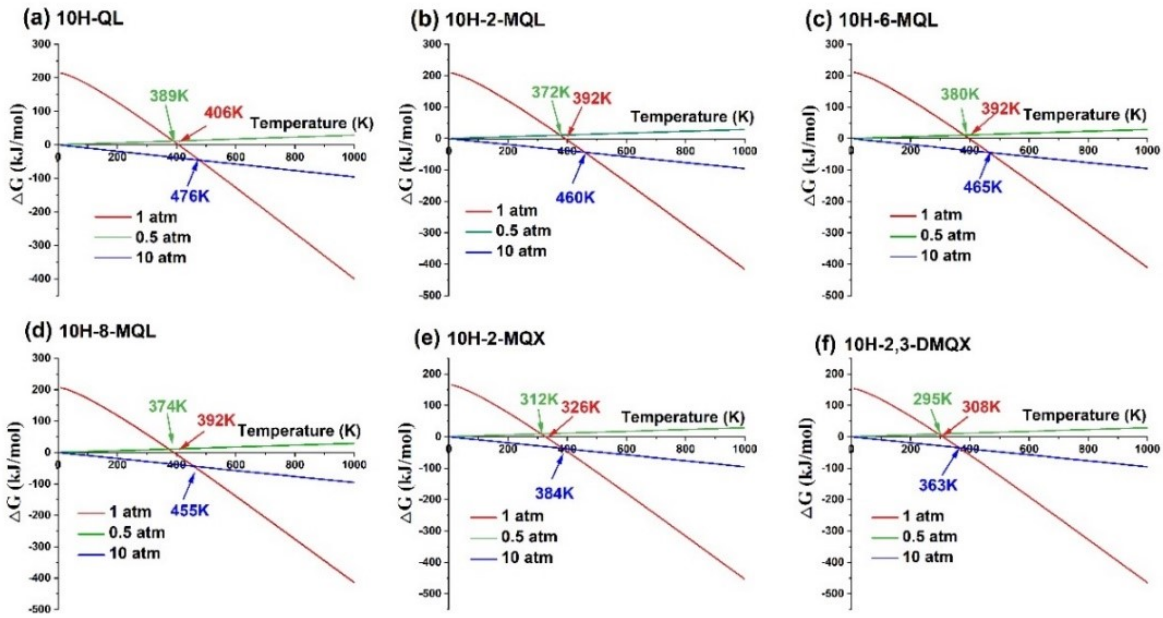

Figure S1. The theoretical dehydrogenation temperatures of Quinoxaline-based Liquid Organic Hydrogen Carriers calculated under different H_2 pressures.

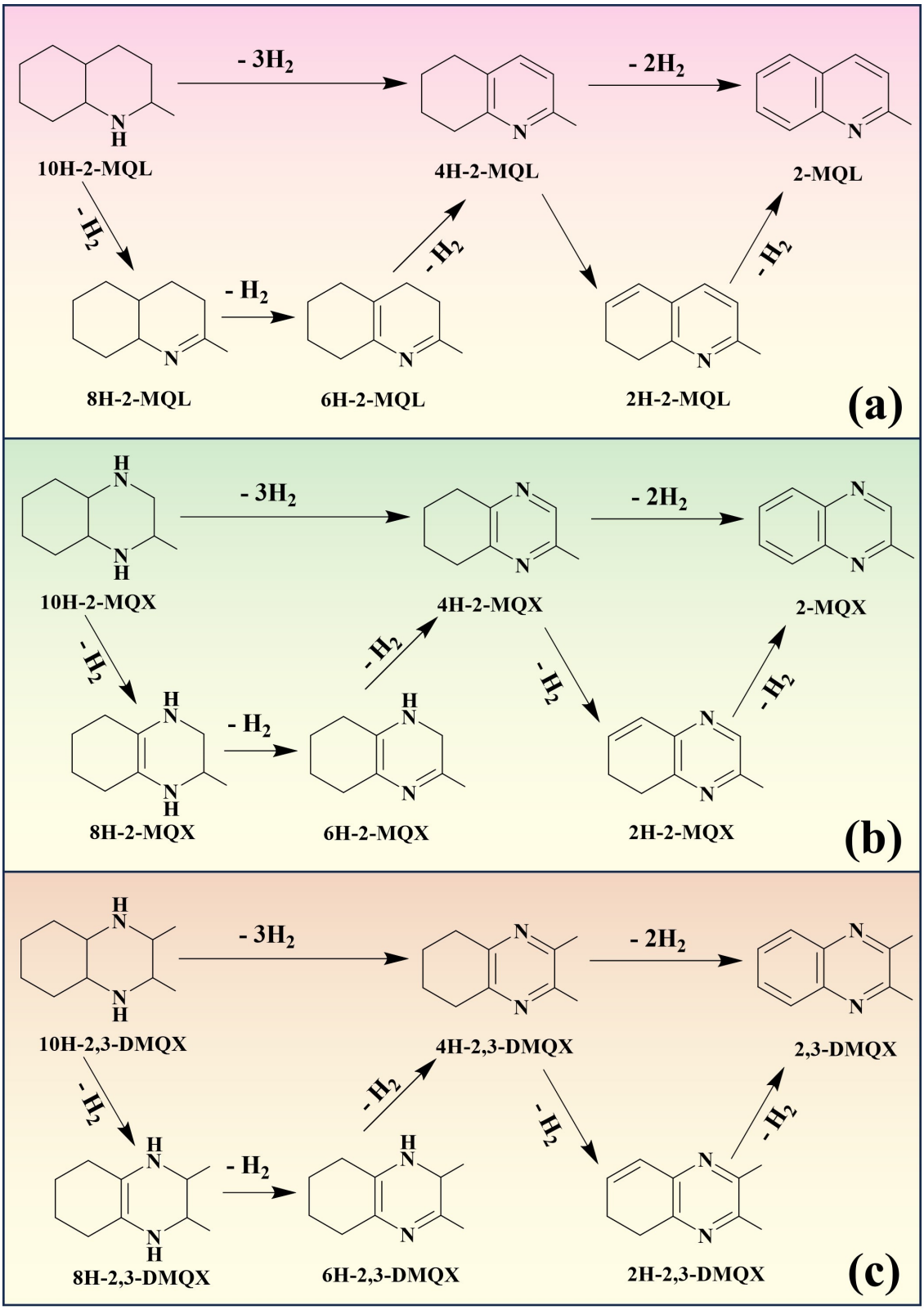

Figure S2. Possible dehydrogenation reaction pathways of 10H-2-MQL, 10H-2-MQX, and 10H-2,3-DMQX.

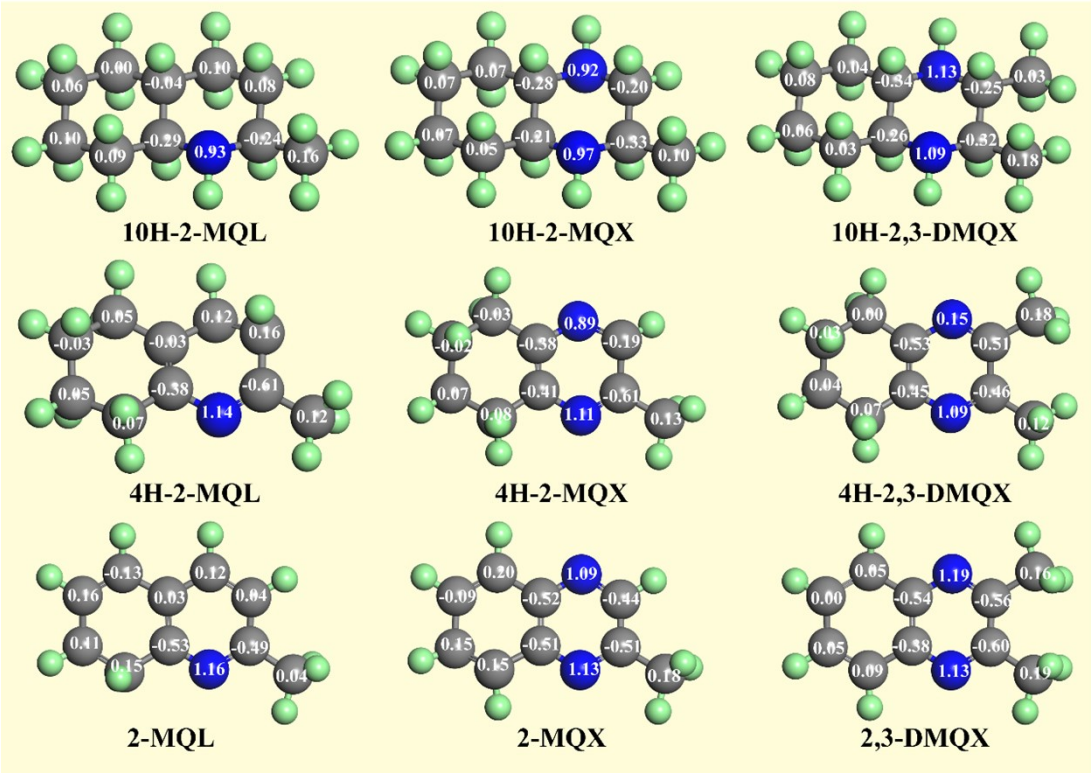

Figure S3. Bader charge of the stable molecular structure of 10H-X, 4H-X, X (X = 2-MQL, 2-MQX, 2,3-DMQX).

Table S1. Hydrogen storage density, dehydrogenation temperatures with different H_2 partial pressures and hydrogen heat of selected quinoxaline-derives.

Molecules	Hydrogen storage density (wt%)	Dehydrogenation temperature (K)			Hydrogenation heat (kJ/mol)
		1 atm[a]	0.5 atm[a]	10 atm[a]	
QL	7.19	331	316	387	-77.32
2-MQL	6.54	392	372	460	-76.50
6-MQL	6.54	392	380	465	-76.81
8-MQL	6.54	392	374	455	-75.87
2-MQX	6.49	326	312	384	-67.90
2,3-DMQX	5.95	308	295	363	-65.66

[a]: partial pressure of H_2.

Table S2. Dehydrogenation performance comparisons of selected LOHCs.

Series	LOHCs	Structural formula	Hydrogen capacity (wt%)	Conditions and performance
Carbazoles	N-ethylcarbazole	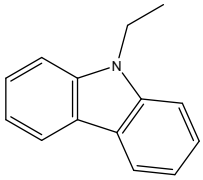	5.79	Pd/Al_2O_3, 180 °C, 101 kPa, 7 h, 80.1% dehydrogenation degree[3]
	N-propylcarbazole	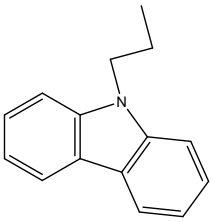	5.43	Pd/Al_2O_3, 180 °C, 101 kPa, 7 h, 80.1% dehydrogenation[4]
Indoles	N-methylindole	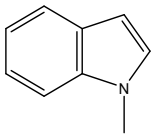	5.76	Pd/Al_2O_3, 190 °C, 101 kPa, 4h, 100% dehydrogenation[5]
	2-methylindole	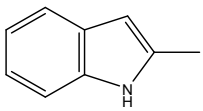	5.76	Pd/Al_2O_3, 190 °C, 101 kPa, 4 h, 100% dehydrogenation in decalin solvent[6]
	1,2-methylindole	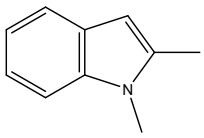	5.23	Pd/Al_2O_3, 200 °C, 101 kPa, 60 min, 100% dehydrogenation in decalin solvent[7]
Quinoxalines	2-methylquinoline	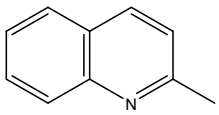	6.53	Pd/Al_2O_3, 200 °C, 101 kPa, 3 h, 25.29% dehydrogenation, **this study**
	2-methylquinoxaline	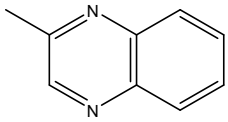	6.49	Pd/Al_2O_3, 200 °C, 101 kPa, 3 h, 81.42% dehydrogenation, **this study**
	2,3-dimethylquinoxaline	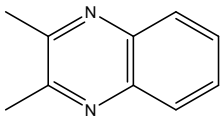	5.95	Pd/Al_2O_3, 200 °C, 101 kPa, 3 h, 89.6% dehydrogenation, **this study**

Table S3. Possible geometry configurations and energies of various isomers of 2-MQL calculated by Materials Studio.

Code	**10H-2-MQL**	**2-MQL**		
Structural formula	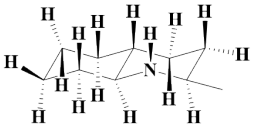	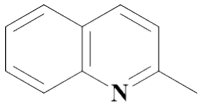		
Energy (eV)	-169.517	-131.621		
Code	**8H-2-MQL(1)**	**8H-2-MQL(2)**	**8H-2-MQL(3)**	**8H-2-MQL(4)**
Structural formula	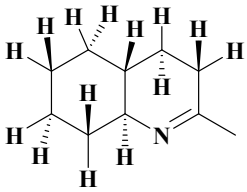	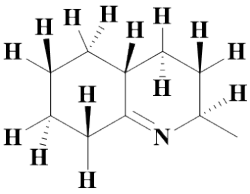	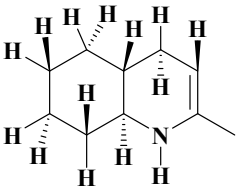	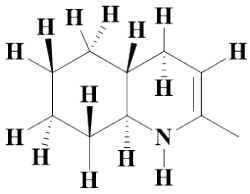
Energy (eV)	-161.624	-161.619	-161.611	-161.613
Code	**8H-2-MQL(5)**	**8H-2-MQL(6)**	**8H-2-MQL(7)**	**8H-2-MQL(8)**
Structural formula	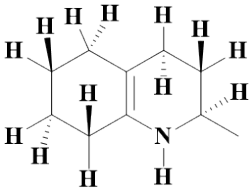	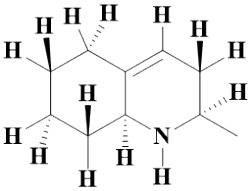	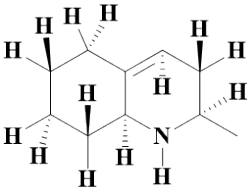	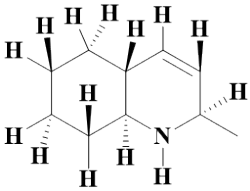
Energy (eV)	-161.366	-161.318	-161.319	-161.190
Code	**8H-2-MQL(9)**	**8H-2-MQL(10)**	**8H-2-MQL(11)**	**8H-2-MQL(12)**
Structural formula	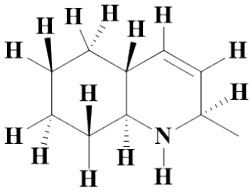	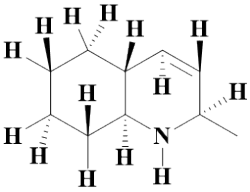	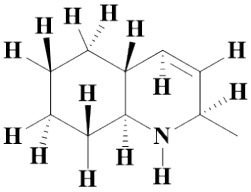	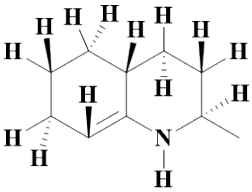

Energy (eV)	-161.190	-159.037	-161.190	-161.528
Code	**8H-2-MQL(13)**	**8H-2-MQL(14)**	**8H-2-MQL(15)**	**8H-2-MQL(16)**
Structural formula	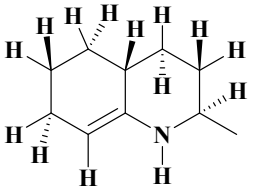	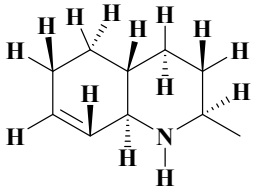	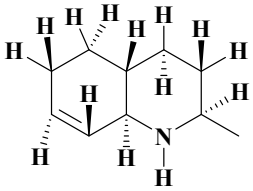	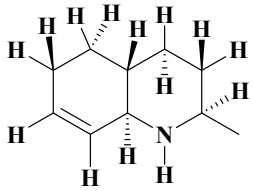
Energy (eV)	-161.526	-161.200	-159.121	-161.199
Code	**8H-2-MQL(17)**	**8H-2-MQL(18)**	**8H-2-MQL(19)**	**8H-2-MQL(20)**
Structural formula	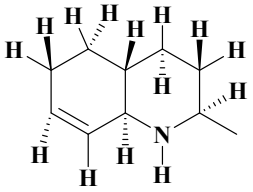	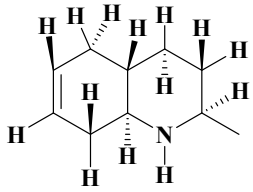	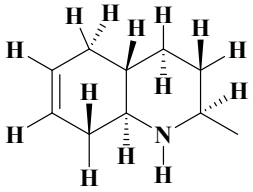	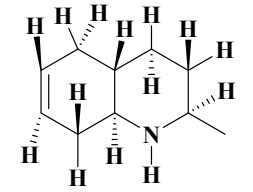
Energy (eV)	-161.200	-161.278	-161.278	-159.016
Code	**8H-2-MQL(21)**	**8H-2-MQL(22)**	**8H-2-MQL(23)**	**8H-2-MQL(24)**
Structural formula	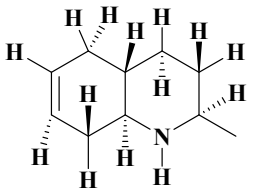	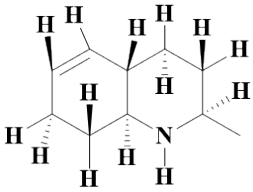	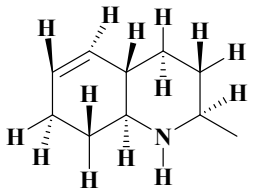	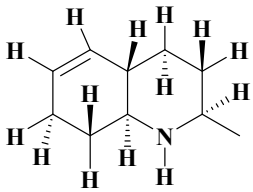
Energy (eV)	-161.278	-161.246	-159.023	-161.244
Code	**8H-2-MQL(25)**	**8H-2-MQL(26)**	**8H-2-MQL(27)**	
Structural formula	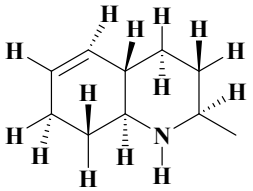	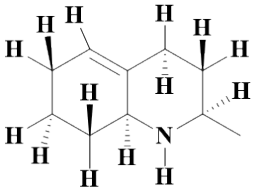	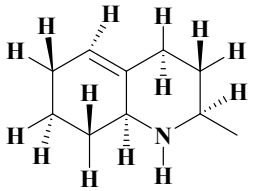	

Energy (eV)	-161.245	-161.291	-161.292	

Code	**6H-2-MQL(1)**	**6H-2-MQL(2)**	**6H-2-MQL(3)**	**6H-2-MQL(4)**
Structural formula	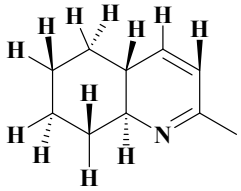	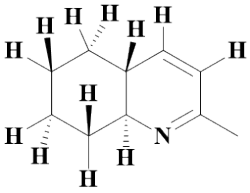	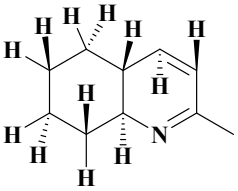	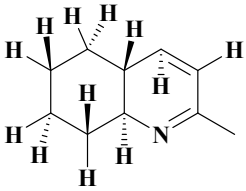
Energy (eV)	-153.485	-153.486	-151.014	-153.487

Code	**6H-2-MQL(5)**	**6H-2-MQL(6)**	**6H-2-MQL(7)**	**6H-2-MQL(8)**
Structural formula	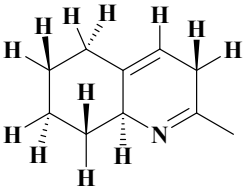	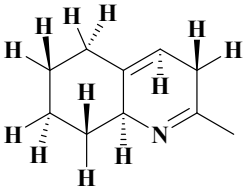	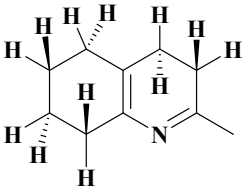	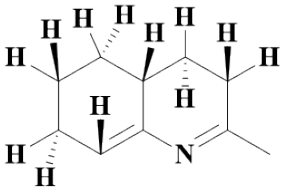
Energy (eV)	-153.579	-153.579	-153.725	-153.725

Code	**6H-2-MQL(9)**	**6H-2-MQL(10)**	**6H-2-MQL(11)**	**6H-2-MQL(12)**
Structural formula	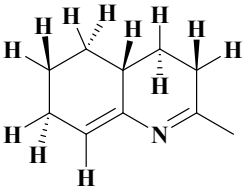	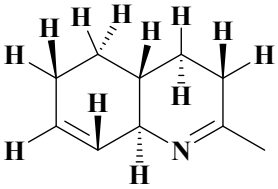	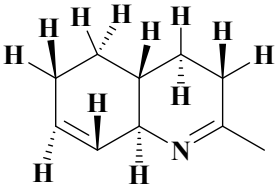	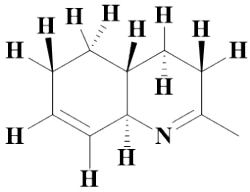
Energy (eV)	-153.725	-153.351	-151.208	-153.351

Code	**6H-2-MQL(13)**	**6H-2-MQL(14)**	**6H-2-MQL(15)**	**6H-2-MQL(16**
Structural formula	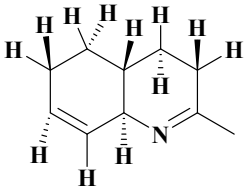	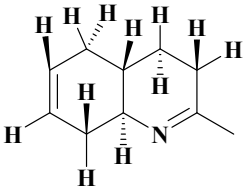	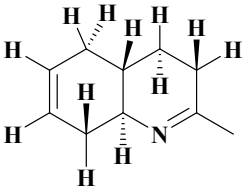	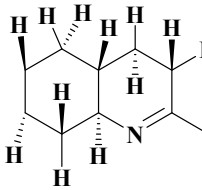

Energy (eV)	-153.349	-153.436	-153.436	-151.145

Code	**6H-2-MQL(17)**	**6H-2-MQL(18)**	**6H-2-MQL(19)**	**6H-2-MQL(20**
Structural formula	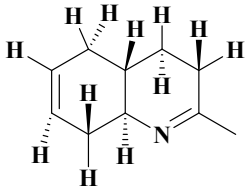	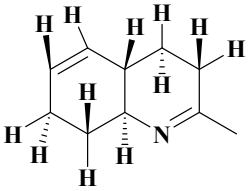	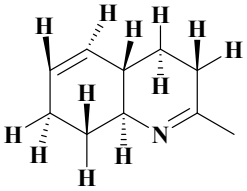	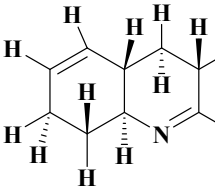
Energy (eV)	-153.436	-153.376	-151.184	-153.377

Code	**6H-2-MQL(21)**	**6H-2-MQL(22)**	**6H-2-MQL(23)**
Structural formula	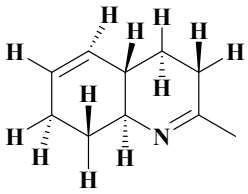	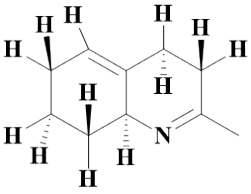	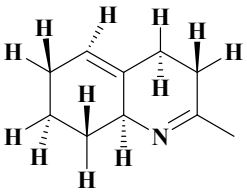
Energy (eV)	-153.377	-153.500	-153.500

Code	4H-2-MQL(1)	**4H-2-MQL(2)**	**4H-2-MQL(3)**	**4H-2-MQL(4)**
Structural formula	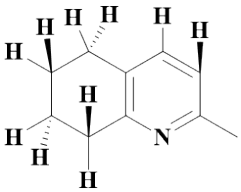	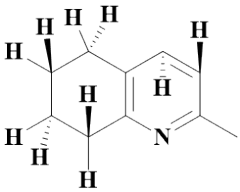	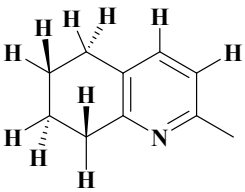	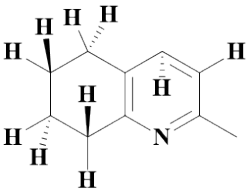
Energy (eV)	-146.841	-142.791	-146.839	-146.839

Code	**4H-2-MQL(5)**	**4H-2-MQL(6)**	**4H-2-MQL(7)**	**4H-2-MQL(8)**
Structural formula	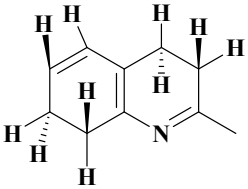	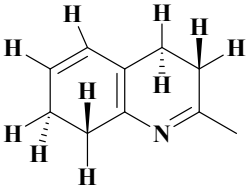	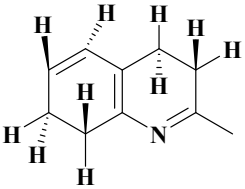	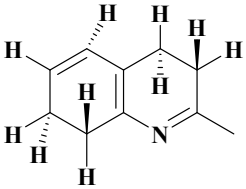
Energy	-145.621	-145.620	-143.169	-145.621

(eV)				
Code	**4H-2-MQL(9)**	**4H-2-MQL(10)**	**4H-2-MQL(11)**	**4H-2-MQL(12)**
Structural formula	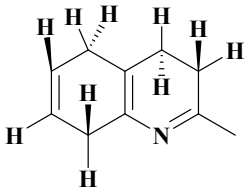	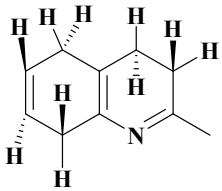	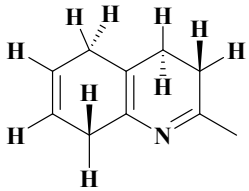	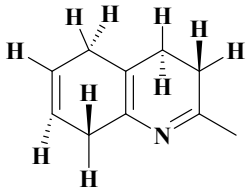
Energy (eV)	-145.566	-143.342	-145.567	-145.567
Code	**4H-2-MQL(13)**	**4H-2-MQL(14)**	**4H-2-MQL(15)**	**4H-2-MQL(16)**
Structural formula	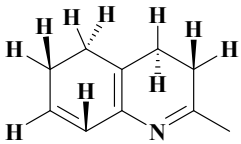	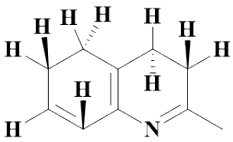	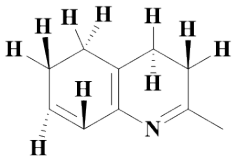	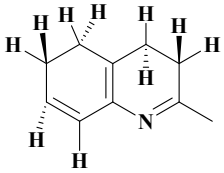
Energy (eV)	-145.570	-145.569	-143.081	-145.570
Code	**2H-2-MQL(1)**	**2H-2-MQL(2)**	**2H-2-MQL(3)**	**2H-2-MQL(4)**
Structural formula	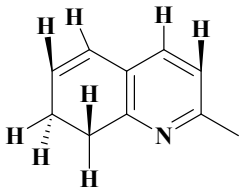	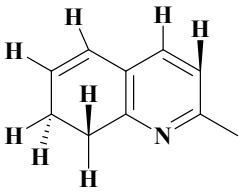	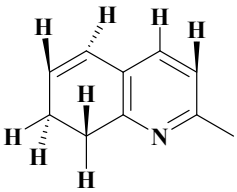	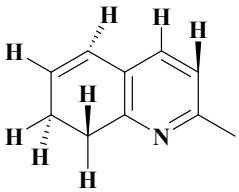
Energy (eV)	-138.772	-138.773	-136.202	-138.772
Code	**2H-2-MQL(5)**	**2H-2-MQL(6)**	**2H-2-MQL(7)**	**2H-2-MQL(8)**
Structural formula	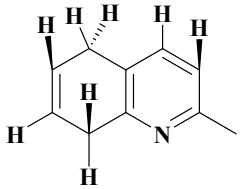	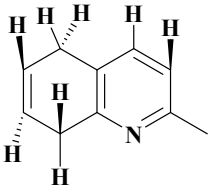	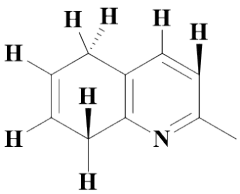	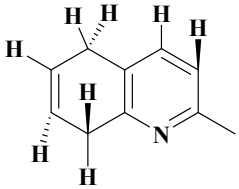
Energy (eV)	-138.645	-136.407	-138.645	-138.647
Code	**2H-2-MQL(9)**	**2H-2-MQL(10)**	**2H-2-MQL(11)**	**2H-2-MQL(12)**

Structural formula	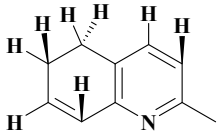	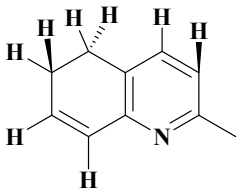	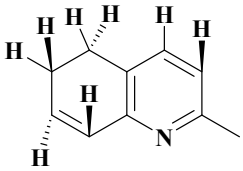	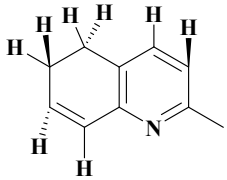
Energy (eV)	-138.751	-138.751	-136.151	-138.752

Table S4. Possible geometry configurations and energies of various isomers of 2-MQX calculated by Materials Studio.

Code	**10H-2-MQX**	**2-MQX**		
Structural formula	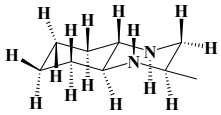	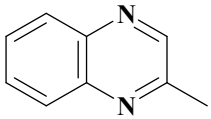		
Energy (eV)	-164.600	-120.897		
Code	**8H-2-MQX(1)**	**8H-2-MQX(2)**	**8H-2-MQX(3)**	**8H-2-MQX(4)**
Structural formula	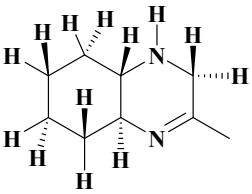	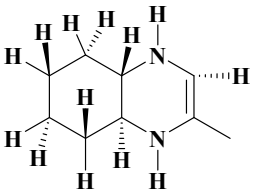	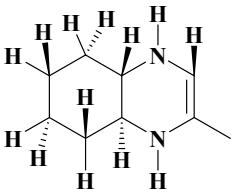	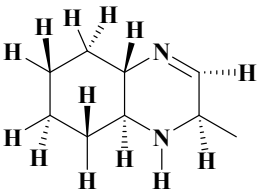
Energy (eV)	-156.726	-156.775	-156.774	-156.573
Code	**8H-2-MQX(5)**	**8H-2-MQX(6)**	**8H-2-MQX(7)**	**8H-2-MQX(8)**
Structural formula	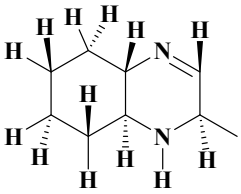	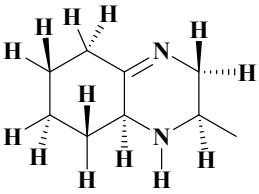	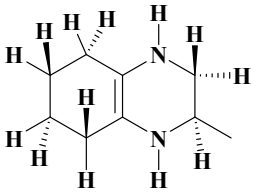	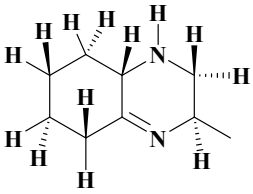

Energy (eV)	-154.844	-156.726	-156.783	-156.69
Code	**8H-2-MQX(9)**	**8H-2-MQX(10)**	**8H-2-MQX(11)**	**8H-2-MQX(12)**
Structural formula	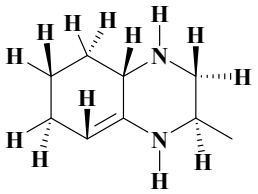	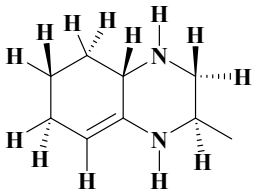	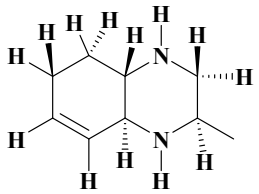	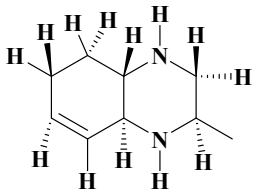
Energy (eV)	-156.567	-156.564	-156.276	-156.277
Code	**8H-2-MQX(13)**	**8H-2-MQX(14)**	**8H-2-MQX(15)**	**8H-2-MQX(16)**
Structural formula	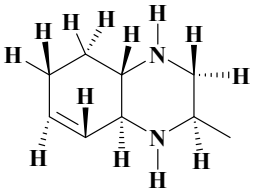	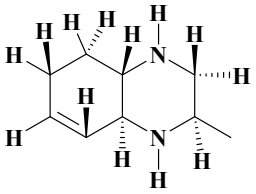	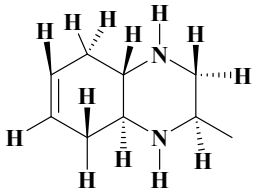	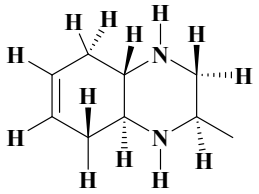
Energy (eV)	-154.135	-156.275	-156.359	-156.358
Code	**8H-2-MQX(17)**	**8H-2-MQX(18)**	**8H-2-MQX(19)**	**8H-2-MQX(20)**
Structural formula	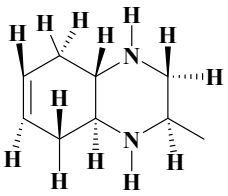	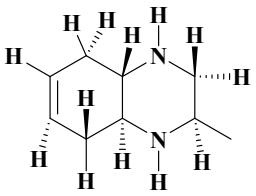	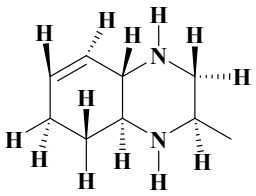	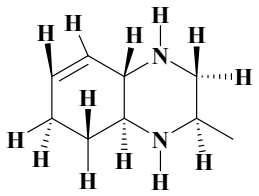
Energy (eV)	-154.040	-156.358	-154.190	-156.176
Code	**8H-2-MQX(21)**	**8H-2-MQX(22)**		

Structural formula	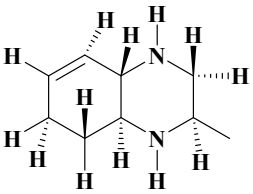	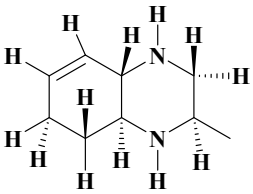		
Energy (eV)	-156.276	-156.276		
Code	**6H-2-MQX(1)**	**6H-2-MQX(2)**	**6H-2-MQX(3)**	**6H-2-MQX(4)**
Structural formula	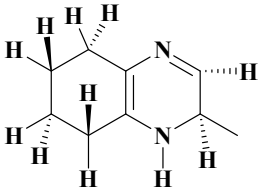	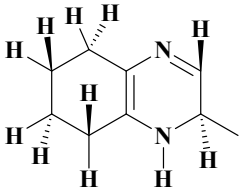	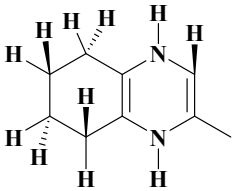	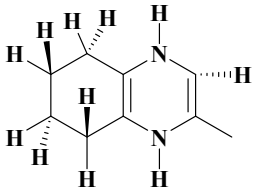
Energy (eV)	-148.885	-148.884	-148.810	-148.805
Code	**6H-2-MQX(5)**	**6H-2-MQX(6)**	**6H-2-MQX(7)**	**6H-2-MQX(8)**
Structural formula	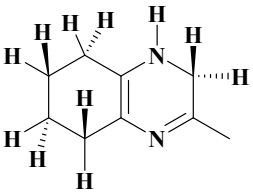	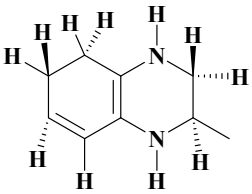	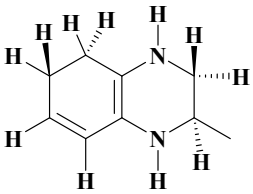	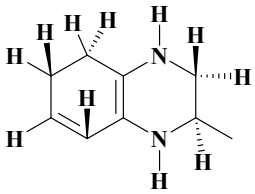
Energy (eV)	-149.031	-148.667	-148.668	-148.666
Code	**6H-2-MQX(9)**	**6H-2-MQX(10)**	**6H-2-MQX(11)**	**6H-2-MQX(12)**
Structural formula	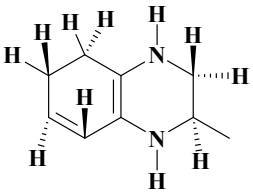	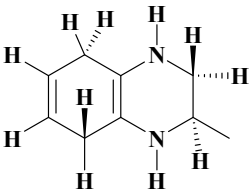	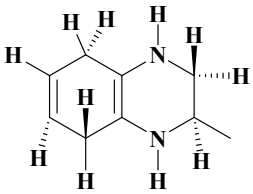	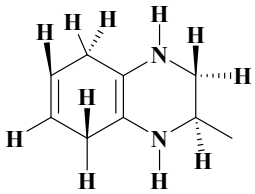
Energy (eV)	-146.505	-148.618	-148.617	-146.497

Code	6H-2-MQX(13)	6H-2-MQX(14)	6H-2-MQX(15)	6H-2-MQX(16)
Structural formula	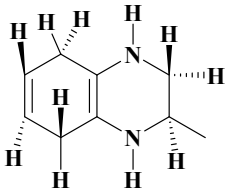	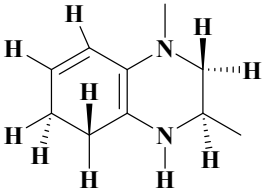	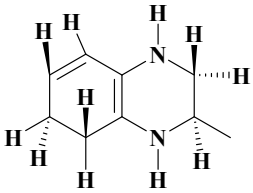	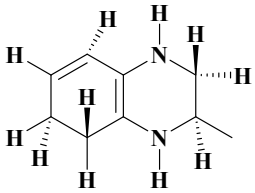
Energy (eV)	-148.619	-146.502	-148.665	-148.664

Code	6H-2-MQX(17)
Structural formula	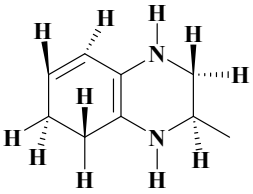
Energy (eV)	-148.664

Code	4H-2-MQX(1)	4H-2-MQX(2)	4H-2-MQX(3)	4H-2-MQX(4)
Structural formula	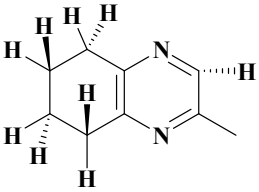	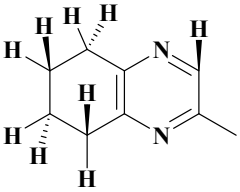	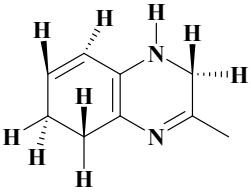	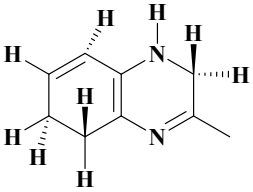
Energy (eV)	-142.097	-142.096	-138.598	-140.888

Code	4H-2-MQX(5)	4H-2-MQX(6)	4H-2-MQX(7)	4H-2-MQX(8)
Structural formula	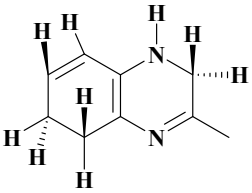	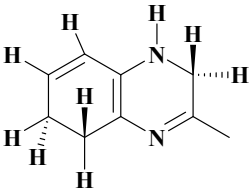	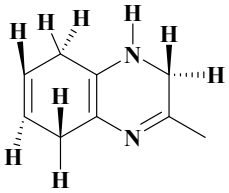	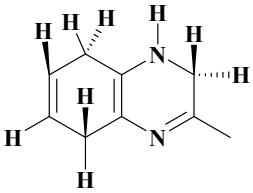
Energy	-140.889	-140.889	-138.794	-140.873

(eV)				
Code	**4H-2-MQX(9)**	**4H-2-MQX(10)**	**4H-2-MQX(11)**	**4H-2-MQX(12)**
Structural formula	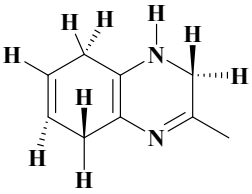	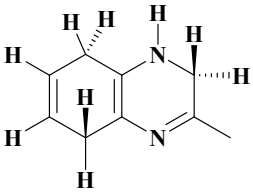	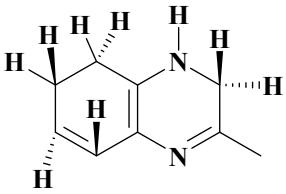	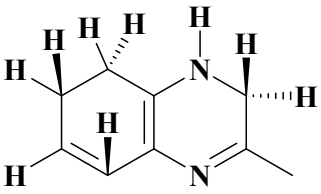
Energy (eV)	-140.874	140.874	-138.523	-140.977
Code	**4H-2-MQX(13)**	**4H-2-MQX(14)**		
Structural formula	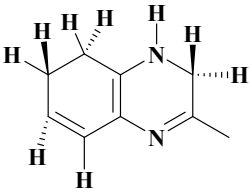	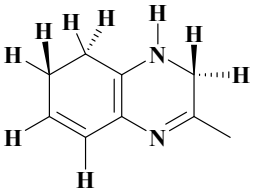		
Energy (eV)	-140.976	-140.976		
Code	**2H-2-MQX(1)**	**2H-2-MQX(2)**	**2H-2-MQX(3)**	**2H-2-MQX(4)**
Structural formula	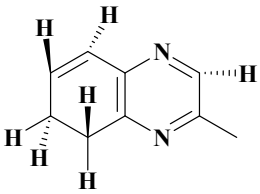	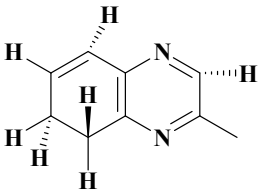	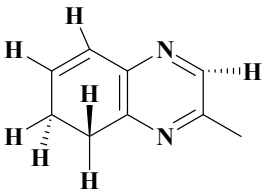	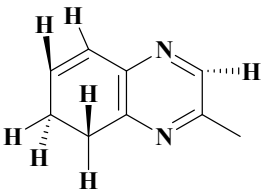
Energy (eV)	-131.397	-133.999	-133.998	-133.997
Code	**2H-2-MQX(5)**	**2H-2-MQX(6)**	**2H-2-MQX(7)**	**2H-2-MQX(8)**
Structural formula	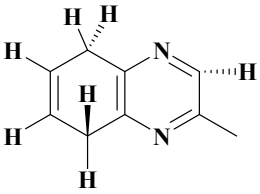	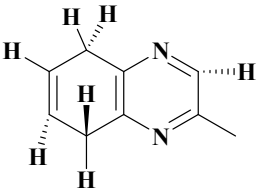	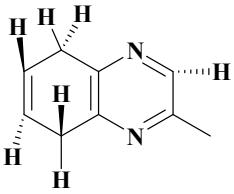	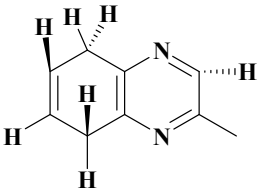

Energy (eV)	-133.905	-133.895	-131.635	-133.900
Code	**2H-2-MQX(9)**	**2H-2-MQX(10)**	**2H-2-MQX(11)**	**2H-2-MQX(12)**
Structural formula	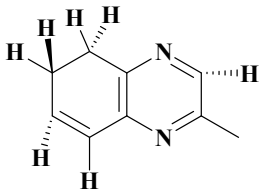	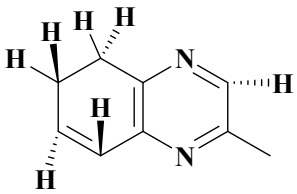	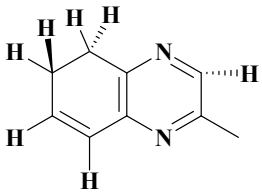	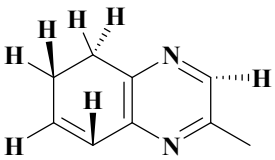
Energy (eV)	-133.997	-131.398	-133.997	-133.997

Table S5. Possible geometry configurations and energies of various isomers of 2,3-DMQX calculated by Materials Studio.

Code	**10H-2,3-DMQX**	**2,3-DMQX**		
Structural formula	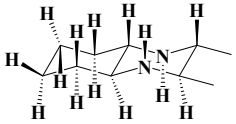	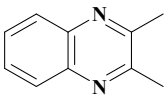		
Energy (eV)	-181.192	-143.562		
Code	**8H-2,3-DMQX(1)**	**8H-2,3-DMQX(2)**	**8H-2,3-DMQX(3)**	**8H-2,3-DMQX (4)**
Structural formula	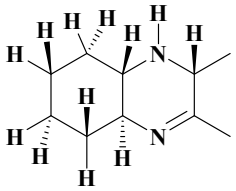	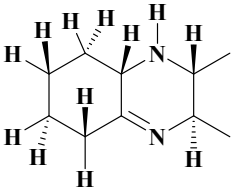	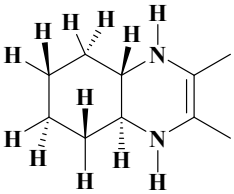	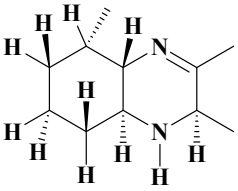
Energy (eV)	-173.285	-173.301	-173.376	-173.286
Code	**8H-2,3-DMQX(5)**	**8H-2,3-DMQX(6)**	**8H-2,3-DMQX(7)**	**8H-2,3-DMQX(8)**

Structural formula	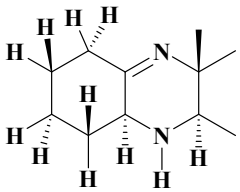	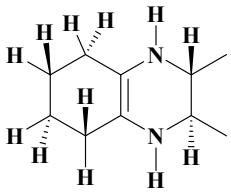	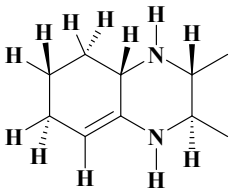	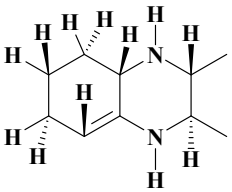
Energy (eV)	-173.299	-173.383	-173.161	-173.163
Code	**8H-2,3-DMQX(9)**	**8H-2,3-DMQX(10)**	**8H-2,3-DMQX(11)**	**8H-2,3-DMQX(12)**
Structural formula	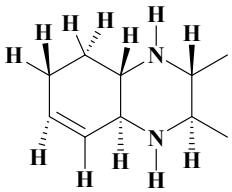	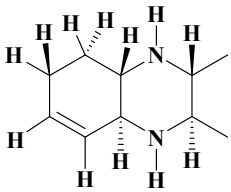	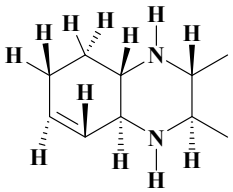	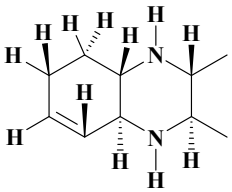
Energy (eV)	-172.867	-172.866	-170.722	-172.866
Code	**8H-2,3-DMQX(13)**	**8H-2,3-DMQX(14)**	**8H-2,3-DMQX(15)**	**8H-2,3-DMQX(16)**
Structural formula	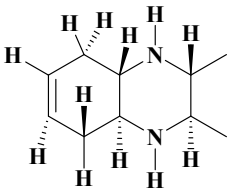	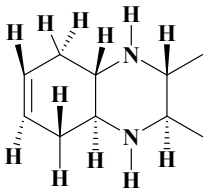	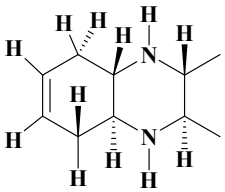	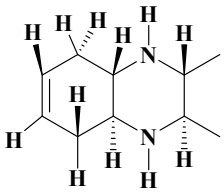
Energy (eV)	-172.952	-170.634	-172.953	-172.953
Code	**8H-2,3-DMQX(17)**	**8H-2,3-DMQX(18)**	**8H-2,3-DMQX(19)**	**8H-2,3-DMQX(20)**
Structural formula	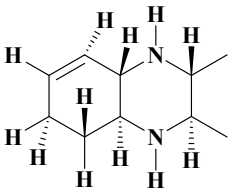	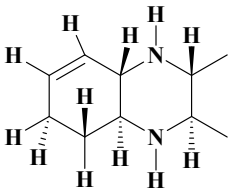	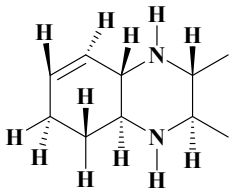	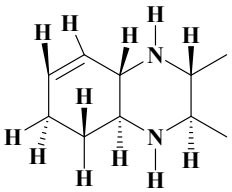
Energy (eV)	-172.867	-172.867	-170.725	-172.867

Code	8H-2,3-DMQX(21)	8H-2,3-DMQX(22)		
Structural formula	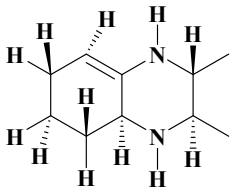	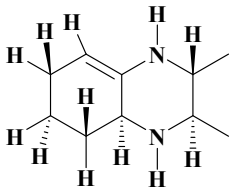		
Energy (eV)	-173.162	-173.163		
Code	**6H-2,3-DMQX(1)**	**6H-2,3-DMQX(2)**	**6H-2,3-DMQX(3)**	**6H-2,3-DMQX(4)**
Structural formula	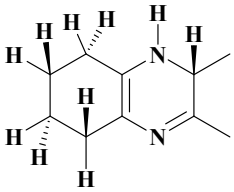	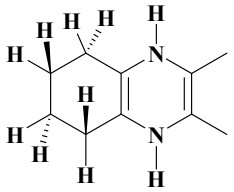	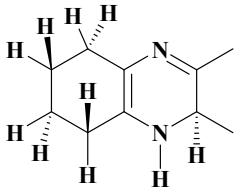	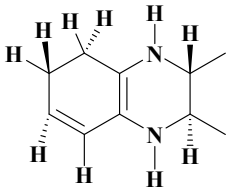
Energy (eV)	-165.610	-165.446	-165.611	-165.268
Code	**6H-2,3-DMQX(5)**	**6H-2,3-DMQX(6)**	**6H-2,3-DMQX(7)**	**6H-2,3-DMQX(8)**
Structural formula	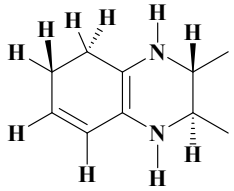	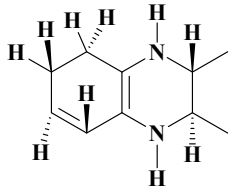	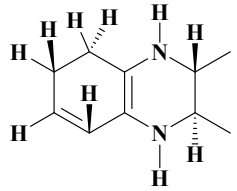	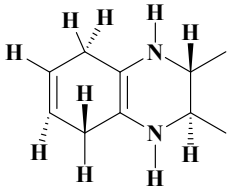
Energy (eV)	-165.268	-163.108	-165.268	-165.220
Code	**6H-2,3-DMQX(9)**	**6H-2,3-DMQX(10)**	**6H-2,3-DMQX(11)**	**6H-2,3-DMQX(12)**
Structural formula	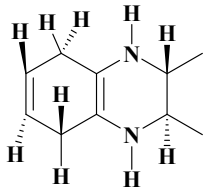	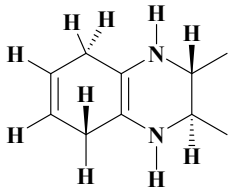	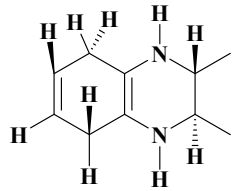	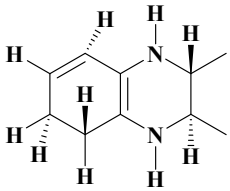
Energy	-163.108	-165.219	-165.218	-165.269

(eV)				
Code	**6H-2,3-DMQX(13)**	**6H-2,3-DMQX(14)**	**6H-2,3-DMQX(15)**	
Structural formula	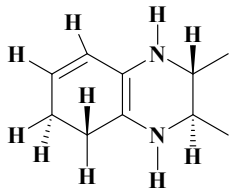	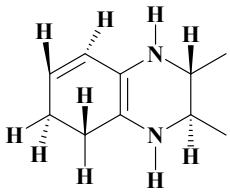	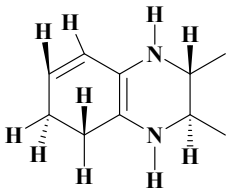	
Energy (eV)	-165.269	-163.115	-165.268	
Code	**4H-2,3-DMQX(1)**	**4H-2,3-DMQX(2)**	**4H-2,3-DMQX(3)**	**4H-2,3-DMQX(4)**
Structural formula	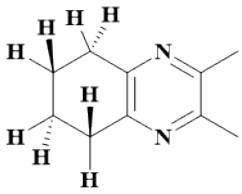	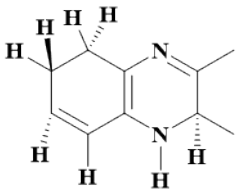	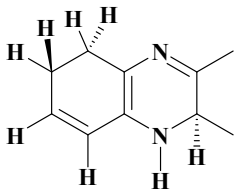	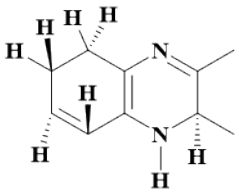
Energy (eV)	-158.823	-157.469	-157.471	-155.179
Code	**4H-2,3-DMQX(5)**	**4H-2,3-DMQX(6)**	**4H-2,3-DMQX(7)**	**4H-2,3-DMQX(8)**
Structural formula	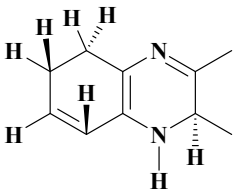	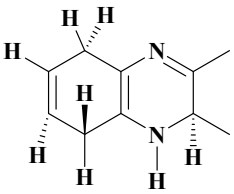	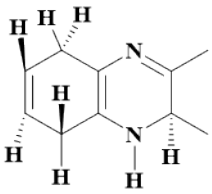	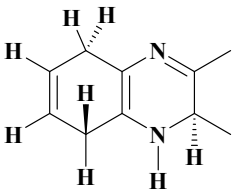
Energy (eV)	-157.469	-157.454	-155.375	-157.452
Code	**4H-2,3-DMQX(9)**	**4H-2,3-DMQX(10)**	**4H-2,3-DMQX(11)**	**4H-2,3-DMQX(12)**
Structural formula	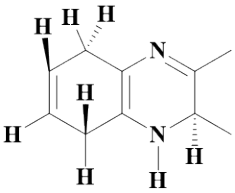	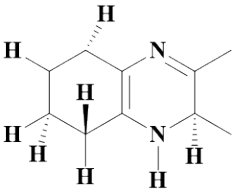	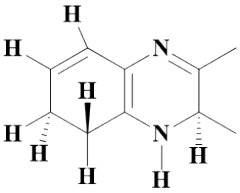	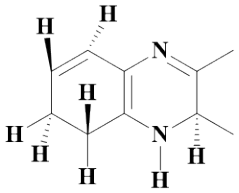

Energy (eV)	-157.453	-157.557	-157.556	-155.099
Code	**4H-2,3-DMQX(13)**			
Structural formula	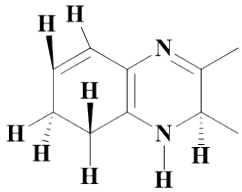			
Energy (eV)	-157.554			
Code	**2H-2,3-DMQX(1)**	**2H-2,3-DMQX(2)**	**2H-2,3-DMQX(3)**	**2H-2,3-DMQX(4)**
Structural formula	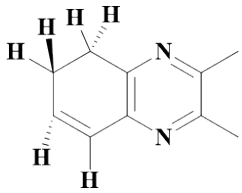	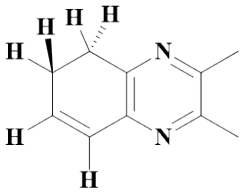	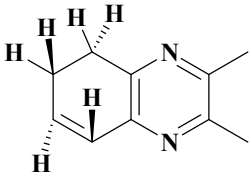	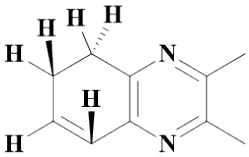
Energy (eV)	-150.723	-150.723	-148.135	-150.724
Code	**2H-2,3-DMQX(5)**	**2H-2,3-DMQX(6)**	**2H-2,3-DMQX(7)**	**2H-2,3-DMQX (8)**
Structural formula	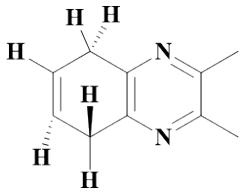	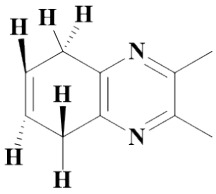	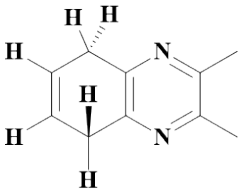	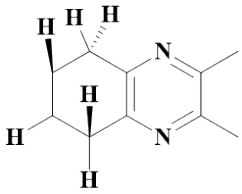
Energy (eV)	-150.632	-148.365	-150.632	-150.627
Code	**2H-2,3-DMQX(9)**	**2H-2,3-DMQX(10)**	**2H-2,3-DMQX(11)**	**2H-2,3-DMQX(12)**

Structural formula	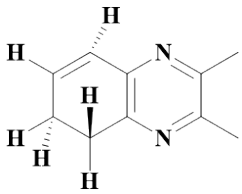	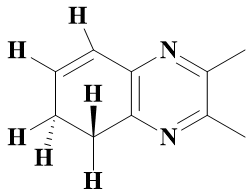	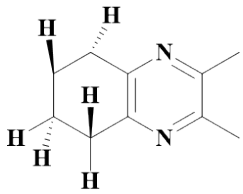	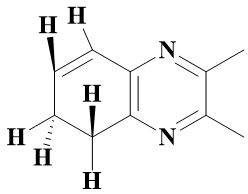
Energy (eV)	-150.722	-150.723	-148.130	-150.720

X	Adsorption energy[a] (eV)			Hydrogenation heat (kJ/mol)	Total reaction energy[b](eV)
	10H-X	4H-X	X		
2-MQL	-1.07	-0.71	-1.82	-76.50	3.92
2-MQX	-1.18	-0.85	-2.17	-67.90	3.85
2,3-DMQX	-1.18	-0.24	-1.82	-65.66	3.81

Table S6**.** Summary of adsorption energy, hydrogenation heat and total reaction energy.

[a]: occurred in X with catalyst surface.

[b]: calculated from 10H-X dehydrogenation to form X.

References:

1. J. Zhou, J. S. Chung and S. G. Kang, *Applied Surface Science*, 2022, **579**, 152142.
2. X. Li, P. Shen, X. Han, Y. Wang, Y. Zhu and Z. Wu, *Applied Surface Science*, 2021, **543**, 148769.
3. B. Wang, T.-y. Chang, Z. Jiang, J.-j. Wei, Y.-h. Zhang, S. Yang and T. Fang, *Int J Hydrogen Energ*, 2018, **43**, 7317-7325.
4. Y. Dong, M. Yang, T. Zhu, X. Chen, G. Cheng, H. Ke and H. Cheng, *ACS Applied Energy Materials*, 2018, **1**, 4285-4292.
5. M. Yang, G. E. Cheng, D. D. Xie, T. Zhu, Y. Dong, H. Z. Ke and H. S. Cheng, *Int J Hydrogen Energ*, 2018, **43**, 8868-8876.
6. L. Li, M. Yang, Y. Dong, P. Mei and H. Cheng, *Int J Hydrogen Energ*, 2016, **41**, 16129-16134.
7. Y. Dong, M. Yang, L. Li, T. Zhu, X. Chen and H. Cheng, *Int J Hydrogen Energ*, 2019, **44**, 4919-4929.